Segregation of alloying atoms at a tilt symmetric grain boundary in tungsten and their strengthening and embrittling effects

2014 Chinese Phys. B 23 106107

(http://iopscience.iop.org/1674-1056/23/10/106107)

Segregation of alloying atoms at a tilt symmetric grain boundary in tungsten and their strengthening and embrittling effects*

Li Zhi-Wu(李志武), Kong Xiang-Shan(孔祥山), Liu-Wei(刘 伟),
Liu Chang-Song(刘长松)†, and Fang Qian-Feng(方前峰)

Key Laboratory of Materials Physics, Institute of Solid State Physics, Chinese Academy of Sciences, Hefei 230031, *China*

(Received 7 November 2013; revised manuscript received 4 April 2014; published online 20 August 2014)

We investigate the segregation behavior of alloying atoms (Sr, Th, In, Cd, Ag, Sc, Au, Zn, Cu, Mn, Cr, and Ti) near Σ3 (111) [1$\bar{1}$0] tilt symmetric grain boundary (GB) in tungsten and their effects on the intergranular embrittlement by performing first-principles calculations. The calculated segregation energies suggest that Ag, Au, Cd, In, Sc, Sr, Th, and Ti prefer to occupy the site in the mirror plane of the GB, while Cu, Cr, Mn, and Zn intend to locate at the first layer nearby the GB core. The calculated strengthening energies predict Sr, Th, In, Cd, Ag, Sc, Au, Ti, and Zn act as embrittlers while Cu, Cr, and Mn act as cohesion enhancers. The correlation of the alloying atom's metal radius with strengthening energy is strong enough to predict the strengthening and embrittling behavior of alloying atoms; that is, the alloying atom with larger metal radius than W acts as an embrittler and the one with smaller metal radius acts as a cohesion enhancer.

Keywords: grain boundary segregation, strengthening and embrittling effect, alloying atom, first-principles calculations

PACS: 61.66.Dk, 61.72.Mm, 28.52.Fa **DOI:** 10.1088/1674-1056/23/10/106107

1. Introduction

Tungsten (W) has some attractive engineering properties, such as high melting temperature, high-temperature strength, good thermal conductivity, and low sputtering erosion. Recently, it has received particular attention as the most promising candidate for various plasma-facing components (PFM), such as the divertor plate in the International Thermonuclear Experimental Reactor (ITER).[1] During its lifetime, the PFM will be submitted to extremely severe conditions: high energy (14 MeV) neutron irradiation, high heat flux, and plasma particle bombardment such as He and H ions.[2,3] These extreme environments can induce property degradation (radiation hardening, embrittlement, swelling, and phase instabilities, and so on).[4–7] Therefore, it is essentially important for W to withstand severe radiation damage.

On the other hand, nano-crystals have been shown to exhibit excellent radiation-tolerance in some cases by experiments of neutrons, protons, and heavy ions, which may render them highly useful for nuclear applications.[8–18] Recently, Bai *et al.*[19] proposed an irradiation-defect self-healing mechanism in copper, suggesting that nano-materials in general might have exceptional radiation resistance. Their interpretation is supported by some previous experiments and suggests new directions for trial materials. With this concept, the manufacture of nano-crystalline W is a remarkable way to improve its radiation-resistant performance. However, nanostructured metals are generally unstable; their grains grow rapidly even at low temperatures, rendering them difficult to process and often unsuitable for usage. This problem seems to be solved by alloying.[20–26] Recently, Chookajorn *et al.*[27] have developed a theoretical framework to design stable nanostructured alloys. They obtained a nanostructure stability map, which is applied to design stable nanostructured tungsten alloys. They identified a candidate alloy, W–Ti, and demonstrated substantially enhanced stability for the high-temperature, long-duration conditions. In addition, according to their study, stable nanocrystalline W alloys can also be synthesized by additions of alloying elements Th, In, Sc, Mn, Zn, Cr, Au. Generally, impurities and alloying additions are aggregated near GBs, modifying the mechanical properties (primarily ductility, fracture toughness, and fracture strength) of metallic materials, and thus poses significant processing and application problems. For example, Nieh presented an evidence of GB segregation of Ni in tungsten using auger electron spectroscopy and demonstrated that such Ni segregation results in a severe embrittlement of tungsten.[28] Aguirre *et al.*[29] found that the GB segregation of Ti improves the mechanical behavior of tungsten with temperature, but makes it more brittle. Murphy *et al.*[30] investigated the mechanical properties of polycrystalline tungsten grown by chemical vapor deposition and found that fluorine segregation to grain boundaries is responsible for the increased brittleness observed in the CVD tungsten. Therefore, it becomes very important to understand the segregation behaviors of these alloying atoms and their strength-

*Project supported by the National Magnetic Confinement Fusion Program (Grant No. 2011GB108004), the National Natural Science Foundation of China (Grant Nos. 91026002 and 91126002), the Strategic Priority Research Program of the Chinese Academy of Sciences (Grant Nos. KJCX2-YW-N35 and XDA03010303), and by the Center for Computation Science, Hefei Institutes of Physical Sciences.

†Corresponding author. E-mail: csliu@issp.ac.cn

ening or embrittling effects on the GB. It is also useful for developing models predicting microstructural and mechanical property changes of engineering metals in nuclear reactors.

First-principles calculations have been very efficient in predicting the embrittling potency of various elements and elucidating the physical mechanisms of the impurity effects. The most common approach is to compare the binding energies of the impurity atoms to the GB and to the surface that would form by cleaving the material along the boundary. It is expected that embrittling impurities should have a stronger binding to the surface than to the GB, with an opposite trend for GB-strengthening elements.[31] A series of first-principles calculations based on this criterion have been done in metals, such as Fe,[32–40] Ni,[41] Mo,[42] Al,[43–45] and Cu,[46] etc. Despite the use of relatively small supercells with simple Σ3 or Σ5 GBs in these works, the predicted embrittlement trends are in good agreement with experimental results. Until now, in tungsten, some works have focused on the segregation behaviors of alloying atoms and their strengthening or embrittling effects on the GB.[47–57] The segregation behavior of some slight elements impurities (such as H, C, N, P, O, S, P, Si, B) in the tungsten grain boundary (Σ3 or Σ5 GBs) are investigated by first-principles and predicted that H, N, O, P, S, Si would weaken the intergranular cohesion in tungsten while B and C improve the intergranular cohesion.[47,49,56,57] The cohesion effect of transition metals on tungsten Σ27 (110) [525] symmetrical tilt grain boundary was studied via first-principles calculations and suggested that the valence of transition metals affect the intergranular cohesion.[55]

In this paper, we investigate the alloying atom's segregation behaviors near a tilt symmetric GB in W and its effect on the intergranular embrittlement by performing first-principles calculations. In this work, the Σ3 (111) $[1\bar{1}0]$ tilt symmetric GB is chosen as a representative example. The alloying elements are chosen from Ref. [27], including Sr, Th, In, Cd, Ag, Sc, Au, Zn, Cu, Mn, Cr, and Ti. Some of them have been identified as candidate alloying elements to obtain stable nanocrystalline W alloys. We will search the stable positions of those alloying elements near the Σ3 (111) $[1\bar{1}0]$ tilt symmetric GB, and estimate the properties of the GB by calculating the adhesive energies.

2. Computational method and details

Our numerical calculations are performed using density functional theory implemented in the Vienna *ab-initio* simulation package (VASP) code.[58,59] The interaction between ions and electrons is described by the projector augmented wave potential (PAW) method.[58] The exchange and correlation functions are taken in a form proposed by Perdew and Wang within the generalized gradient approximation (GGA).[60] The plane wave cutoff and k-point density are both checked for convergence for each system to be within 0.001 eV per atom. Following a series of test calculations, a plane wave cutoff of 450 eV and a k-point grid density of $8 \times 4 \times 1$ are employed. All of the atoms are relaxed until the forces on each of them in our calculations are less than 0.01 eV/Å.

To get accurate results, the slab needs to be thick enough to contain atoms with a bulk-like atomic environment. To determine the necessary thickness, we have calculated the total energy change ($\Delta E_{\rm tot}^{\rm Vac}$) of the GB system when one tungsten atom is removed from the middle site between the GB plane and the surface of the slab. The calculated results are presented in Fig. 1. It can be seen that the total energy change converges to a constant value (∼16.19 eV) when the GB slab number is larger than 21, which is slightly larger than the total energy change (16.12 eV) in bulk when one tungsten atom is removed from the system. Hence, at least 21-layers for the GB slab were required to obtain reliable results. In this work, a 29-layers slab model was adopted to simulate the pure Σ3 (111) $[1\bar{1}0]$ tilt GB. In constructing the GB, we used the theoretical equilibrium lattice parameter of W (3.176 Å).[61] The value has been determined by us previously within GGA, which is in good agreement with the experimental value of 3.165 Å.[62] As sketched in Fig. 2(a), the GB system is composed of two identical grains, each containing 14 layers with one layer on the GB plane shared by the two grains. A vacuum region of 10-Å thickness is added on both sides. The atom belonging to the shared plane and usually designated a "core atom", is marked as site 0 in Fig. 2. The clean GB exhibits mirror symmetry, so sites $-i$ and i ($i = 1 \sim 7$) are equivalent. One alloying atom is placed near the GB core in each unit cell, replacing a W atom. The energetically preferred site (0∼5) for the alloying atom along the GB is then determined. After relaxation of the GB system, the slab representing the free surface (FS) is created by removing the atoms representing the second grain, consisting of 15-layers atoms (see Fig. 2(b)).

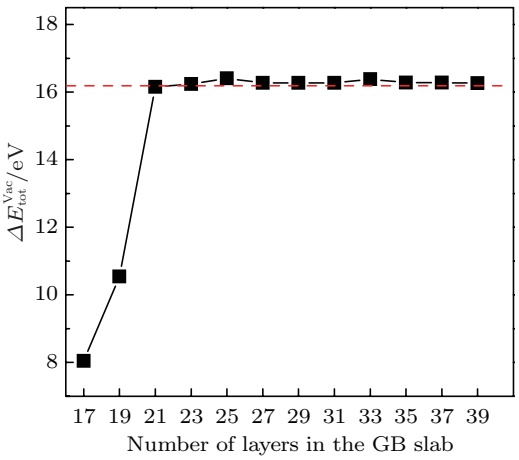

Fig. 1. (color online) The total energy change of the GB system when one tungsten atom is removed from the middle site between the GB plane and the surface of the slab.

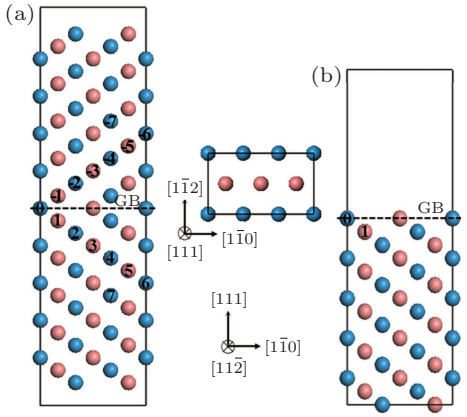

Fig. 2. (color online) Side and top views of the computational cell used to model the Σ3 (111) [1$\bar{1}$0] tilt grain boundary and FS (111) in bcc W. Atoms near the GB and FS are numbered by the atomic layer counted from the GB plane.

3. Result and discussion

3.1. Segregation of alloying atoms near W GB

The tendency of an alloying atom to segregate to an GB is controlled by its segregation energy $E_{\rm seg}$. $E_{\rm seg}$ is the energy required to swap a solute at a bulk position with a W atom at one of the GB positions and can be calculated by

$$E_{\rm seg} = E^{\rm AA}_{\rm GB} - E^{\rm AA}_{\rm Bulk}, \tag{1}$$

where $E^{\rm AA}_{\rm GB}$ is the total energy of the system with a GB and an alloying atom near the GB, and $E^{\rm AA}_{\rm Bulk}$ is the total energy of the system with a GB and an alloying atom in a bulk site. Here, site 7 is chosen as the bulk-like site when calculating $E^{\rm AA}_{\rm Bulk}$ because it has been proved to have a bulk-like local atomic environment (see Fig. 1).

Due to their large atomic size, the alloying atoms prefer to occupy a substitutional site near the GB rather than the GB interstitial site. To identify the most energetically favorable segregation site, six different substitution sites (0∼5) near the GB are considered for calculating the segregation energy. The results are summarized in Fig. 3. According to the segregation energy, the alloying atoms can be divided into two types. The first type of alloying atoms, including Ag, Au, Cd, In, Sc, Sr, Th, and Ti, prefer to occupy the core site in the mirror plane (site 0) of the GB, while the second type of alloying atoms, including Cu, Cr, Mn, and Zn, tend to locate at the site in the first layer (site 1) of the GB. To understand the underlying physical factors controlling the segregation behavior of the alloying atoms, we carefully compared the electronegativity and atomic size of the two types of alloying atoms. We found that the first type of alloying atoms have a larger metallic radius than tungsten, while the second type of alloying atoms have a smaller metallic radius than tungsten. Therefore, the alloying atom with a larger metallic radius prefers to locate at the core site whereas the alloying atom with a smaller one prefers to occupy the site in the first layer of the GB. The segregation energies of all alloying atoms at the stable site in the GB are negative, indicating a driving force for the alloying atom segregation to the GB sites from the bulk. In addition, it can be clearly seen from Fig. 3 that the segregation energies of all alloying atoms converge to zero when the alloying atom locates at the site in the fifth layer (site 5) of the GB, meaning that the GB influences the upper and lower five layers nearby. In other words, the influence range of the GB in W is about ±4.62 Å perpendicular to the GB plane. It can also be seen that the segregation energies do not vary monotonically from layers 1 to 5 for most alloying atoms. Particularly, for Sc and Ti, their segregation energies at the first layer are positive and greatly larger than that at the second layer and the core plane, meaning that the first layer would impede the Sc and Ti segregation on the GB plane.

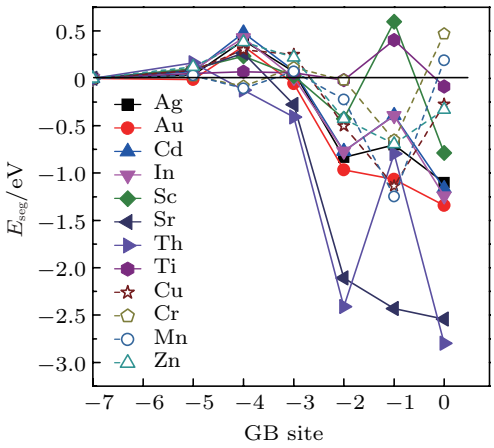

Fig. 3. (color online) The calculated segregation energies (eV) for solutes on the GB i site ($i = 0 \sim 5$).

Based on the above results of the segregation energy, the alloying atom concentration in the GB can be estimated by the McLean equation:[63]

$$C_{\rm GB} = \frac{C_{\rm bulk}\exp\left(-E_{\rm seg}/kT\right)}{1 + C_{\rm bulk}\exp\left(-E_{\rm seg}/kT\right)}, \tag{2}$$

where $E_{\rm seg}$ is the segregation energy of the alloying atom at the stablest site nearby the GB, T is the aging temperature, k is the Boltzmann constant, and $C_{\rm GB}$ and $C_{\rm bulk}$ are the alloying atom concentration in the GB and bulk, respectively. Clearly, the $C_{\rm GB}$ strongly depends on the temperature, the $C_{\rm bulk}$, and the segregation energy. Higher temperatures will lead to a higher bulk concentration and a lower segregation energy, while more alloying atoms can be located at the GB. Here, we chose two typical temperatures: $T = 300$ K, which is the room temperature, and $T = 900$ K, which is in the operating temperature of W as the plasma-facing materials in fusion reactors (800 K–1200 K in ITER and 700 K–1400 K in Demo).[64] We also

chose two concentrations of the alloying atom in bulk, namely 1 appm and 10^4 appm. The low concentration is on the order of the concentration of impurity elements in W,[65] and the high one represents the alloying concentration.

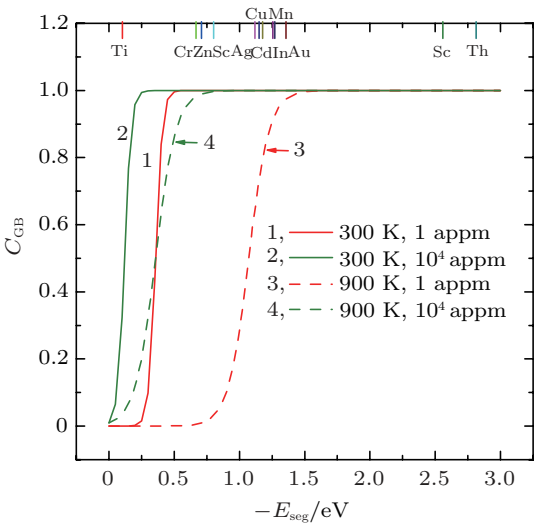

Fig. 4. (color online) The calculated concentration of the alloying atom in the GB sites as a function of the segregation energy at different temperatures and bulk concentrations based on the McLean's equation.

Figure 4 shows the McLean curves for these temperatures and bulk concentrations. On the whole, most alloying atoms will segregate at the W GB within the above temperature and concentration ranges. For example, at room temperature, a segregation energy lower than -0.5 eV will lead to the segregation of all the alloying atoms to the GB, independent of the concentration. The segregation energies of Cr, Zn, Sc, Cd, Cu, Mn, Ag, In, Au, Sr, and Th when occupying the most stable sites in the GB are much lower than -0.5 eV. Consequently, almost all these eleven alloying atoms will be located at the W GB at room temperature and within 1 appm$\sim 10^4$ appm concentration ranges. Similarly, at the operating temperature, the GB will be almost saturated with segregated Cd, Cu, Mn, Ag, In, Au, Sr, and Th within the concentration ranges. However, for Zn, Cr, and Sc, the bulk concentration plays an important role in the separation of the alloying atoms between the bulk and the GB at the operation temperature. Almost all of these three alloying atoms will segregate at the W GB at the higher bulk concentration (10^4 appm) but remain in the bulk at the smaller bulk concentration (1 appm). Of particular note, the C_{GB} values of Ti is very small in the above temperature and concentration ranges due to its large segregation energy (-0.09 eV). When $C_{bulk} = 1$ appm, the equilibrium Ti concentrations in the GB are 33 appm and 3.2 appm at the room and operation temperature, respectively, and when $C_{bulk} = 10^4$ appm, the equilibrium Ti concentrations in the GB are 25×10^4 appm and 3×10^4 appm at the room temperature and operation temperature, respectively. However, these C_{GB} values of Ti are still a few or several times larger than their respective C_{bulk} values.

3.2. Strengthening and embrittling behavior

In the previous sections, on the basis of segregation energy, we predict that Ag, Au, Cd, In, Sc, Sr, Th, and Ti prefer to occupy the core site in the mirror plane of the GB, and Cu, Cr, Mn, and Zn prefer to reside at the site in the first layer nearby the GB core. All of them will segregate at the GB. From these results, it is natural to ask whether an alloying atom is a cohesion enhancer and causes the strengthening of the GB or is an embrittler and induces the weakening of the GB. To answer this question, the strengthening or embrittling effects of alloying atoms on the GB are investigated, which can be quantitatively determined by the strengthening energy (ΔE_{SE}). According to the Rice–Wang model,[66] it can be defined as the difference between the binding energies of an alloying atom at the GB ($\Delta E_{GB} = E_{GB}^{AA} - E_{GB} - E_{AA}$) and FS ($\Delta E_{FS} = E_{FS}^{AA} - E_{FS} - E_{AA}$). Here, E_{GB} and E_{FS} are the total energy of the clean GB and FS slab, respectively, and E_{FS}^{AA} is the total energy the FS system with an alloying atom, and E_{AA} is the total energy of an isolated alloying atom. Thus, the strengthening energy can be written as

$$\Delta E_{SE} = E_{GB}^{AA} - E_{GB} - (E_{FS}^{AA} - E_{FS}). \quad (3)$$

A negative value of ΔE_{SE} means enhancement of the GB cohesion, while a positive value corresponds to embrittlement.

The strengthening energies of the alloying atoms at their stablest site are calculated and summarized in Fig. 5. The results suggest that Sr, Th, In, Cd, Ag, Sc, Au, Ti, and Zn are embrittlers and Cu, Cr, Mn as cohesion enhancers. For other sites, similar conclusion can be obtained. As shown in Fig. 5, whether occupying the site 0 or 1, Sr, Th, In, Cd, Ag, Sc, Au, Ti, and Zn are embrittlers. For the case of Cu, Cr, Mn, these three elements are cohesion enhancers when they are placed at the site 1 and cohesion embrittlers when they are placed at the site 0. For site 2, all of the strengthening energies are almost zero, suggesting that these elements in site 2 have almost no influence on the mechanical properties of the grain boundary. It should be noted that the segregation energy of Cr and Mn at site 0 are 0.47 eV and 0.19 eV, respectively. This means that site 0 is an energetically unfavorable site for the Cr and Mn. The segregation energy of Cu at site 0 are greatly larger than that at site 1, about 1 eV. According to the site-competition effect, as a result of which the site with a lower energy tends to replace the site with higher energy, the segregation concentration of Cu, Cr, and Mn at the site 0 can be negligible compared to at their stable site. Hence, it is reliable that Sr, Th, In, Cd, Ag, Sc, Au, Ti, and Zn are embrittlers and Cu, Cr, Mn as cohesion enhancers.

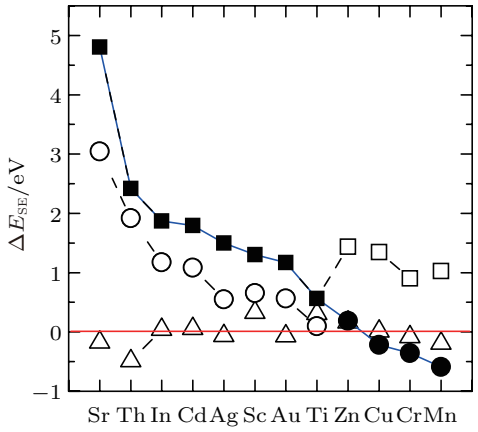

Fig. 5. (color online) The calculated strengthening energy for GB in W doped with alloying atom placed at site 0, 1, and 2. They are denoted by square, circle, and triangle, respectively. The solid square and circle present the strengthening energy of these alloying atoms at their stablest sites.

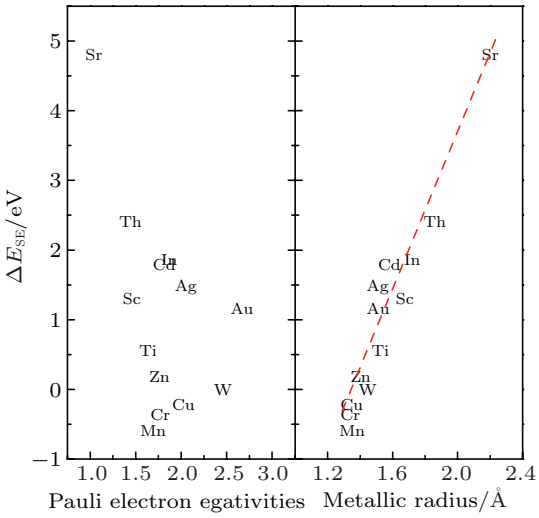

Fig. 6. (color online) The correlation of the strengthening energy with the metal radius of alloying atoms and Pauli electrongativities.

It has been shown that the GB embrittlement is a consequence of changes in the bonding at GB, which can be explained by the mechanical effect, related to the atomic size of the alloying additions or the chemical mechanism, which is encompassed in the electron redistribution, determined by the propensity for a particular alloying atom to gain or lose electron. Generally, the propensity is characterized by the electronegativity. Hence, to explore whether the strengthening and embrittling effect is primarily a geometric or electronic effect, we have plotted the connection between ΔE_{SE} and the metal radius of the alloying atom (as a measure of the geometric effect) and the Pauli electronegativity (as a measure of the electronic effect). As shown in Fig. 6, the correlation of the ΔE_{SE} with Pauli electronegativity is invisible, while that with metal radius is evident and positive. This means that the strengthening and embrittling effects of the alloying atom are dominated by the geometric effect. The correlation between the ΔE_{SE} and the metal radius is efficient enough to be used as an indicator for the strengthening and embrittling behaviors of alloying atom; that is, the alloying atom with larger metal radius than W acts as a embrittler for W $\Sigma 3$ (111) GB and the alloying atom with smaller metal radius than W acts as a cohesion enhancer. Small/large atoms tend to enhance/decrease the grain boundary cohesion may because it reduces/increases the internal stress suffered by GB1 and GB-1 atom pair across the boundary. However, this correlation between atomic size and embrittling effect of an alloying element still needs to be further checked due to a few alloying element species in this work.

4. Conclusion

In this paper, we have investigated the alloying atom's (Sr, Th, In, Cd, Ag, Sc, Au, Zn, Cu, Mn, Cr, and Ti) segregation behaviors near $\Sigma 3$ (111) $[1\bar{1}0]$ the symmetric GB in W and their effect on the intergranular embrittlement by performing first-principles calculations. Firstly, the segregation energy was calculated to find out which site the alloying atom prefers to occupy. The calculated segregation energies suggest that Ag, Au, Cd, In, Sc, Sr, Th, and Ti prefer to occupy the core site in the mirror plane of the GB, and Cu, Cr, Mn, and Zn prefer to reside at the site in the first layer nearby the GB core. Based on the segregation energy, the alloying atom concentration in the GB is discussed according to the McLean equation. We found that, for most alloying elements, almost all of the alloying atoms will be located at the W GB in the ranges of 300 K–900 K and 1 appm–10^{-4} appm. Then, the strengthening or embrittling effects of the alloying atom on the GB are investigated by calculating the strengthening energy. We found that the Sr, Th, In, Cd, Ag, Sc, Au, Ti, and Zn act as embrittlers and Cu, Cr, and Mn act as cohesion enhancers. The strengthening energy is positively correlated with the metal radius; that is, a larger metal radius will lead to a bigger strengthening energy, while the correlation of the strengthening energy with Pauli electronegativity is invisible. These results indicate that the strengthening and embrittling effects of the alloying atom are dominated by the geometric effect.

References

[1] Causey R, Wilson K, Venhaus T and Wampler W R 1999 *J. Nucl. Mater.* **266** 467
[2] Lee H T, Haasz A A, Davis J W and Macaulay-Newcombe R G 2007 *J. Nucl. Mater.* **360** 196
[3] Davis J W, Barabash V R, Makhankov A, Plöchl L and Slattery K T 1998 *J. Nucl. Mater.* **258** 308
[4] Behrisch R and Venus G 1993 *J. Nucl. Mater.* **202** 1
[5] Smid I, Akiba M, Vieider G and Plöchl L 1998 *J. Nucl. Mater.* **258–263** 160
[6] Fujitsuka M, Mutoh I, Tanabe T and Shikama T 1996 *J. Nucl. Mater.* **233–237** 638

[7] Pacher H D, Smid I, Federici G, Igitkhanov Yu, Janeschitz G, Raffray R and Vieider G 1997 *J. Nucl. Mater.* **241–243** 255
[8] Lu K, Lu L and Suresh S 2009 *Science* **324** 349
[9] Weertman J R, Farkas D, Hemker K, Kung H, Mayo M, Mitra R and Van Swygenhoven H 1999 *MRS Bull.* **24** 44
[10] Swygenhoven H V and Weertman J R 2006 *Mater. Today* **9** 24
[11] Liao X Z, Zhou F, Lavernia E J, He D W and Zhu Y T 2003 *Appl. Phys. Lett.* **83** 5062
[12] Lu L, Sui M L and Lu K 2000 *Science* **287** 1463
[13] Lu L, Shen Y, Chen X, Qian L and Lu K 2004 *Science* **304** 422
[14] Wang Y, Chen M, Zhou F and Ma E 2002 *Nature* **419** 912
[15] Witkin D B and Lavernia E J 2006 *Prog. Mater. Sci.* **51** 1
[16] Poudel B *et al.* 2008 *Science* **320** 634
[17] McHenry M E, Willard M A and Laughlin D E 1999 *Prog. Mater. Sci.* **44** 291
[18] Ackland G 2010 *Science* **327** 1587
[19] Bai X M, Voter A F, Hoagland R G, Nastasi M and Uberuaga B P 2010 *Science* **327** 1631
[20] Weissmüller J 1993 *Nanostruct. Mater.* **3** 261
[21] Kirchheim R 2002 *Acta Mater.* **50** 413
[22] Kirchheim R 2007 *Acta Mater.* **55** 5129
[23] Kirchheim R 2007 *Acta Mater.* **55** 5139
[24] Millett P C, Selvam R P and Saxena A 2007 *Acta Mater.* **55** 2329
[25] Luo J, Cheng H, Asl K M, Kiely C J and Harmer M P 2011 *Science* **333** 1730
[26] Baram M, Chatain D and Kaplan W D 2011 *Science* **332** 206
[27] Chookajorn T, Murdoch H A and Schuh C A 2012 *Science* **337** 951
[28] Nieh T G 1984 *Scr. Metall.* **18** 1279
[29] Aguirre M V, Martin A, Pastor J Y, LLorca J, Monge M A and Pareja R 2011 *J. Nucl. Mater.* **417** 516
[30] Murphy J D, Giannattasio A, Yao Z, Hetherington C J D, Nellist P D and Roberts S G 2009 *J. Nucl. Mater.* **386–388** 583
[31] Mishin Y, Asta M and Li J 2010 *Acta Mater.* **58** 1117
[32] Wachowicz E, Ossowski T and Kiejna A 2010 *Phys. Rev. B* **81** 094104
[33] Geng W T, Freeman A J and Olson G B 2001 *Phys. Rev. B* **63** 165415
[34] Bhattacharya S K, Tanaka S, Shiihara Y and Kohyama M 2013 *J. Phys.: Condens. Matter* **25** 135004
[35] Wu R, Freeman A J and Olson G B 1994 *Phys. Rev. B* **50** 75
[36] Wu R, Freeman A J and Olson G B 1996 *Phys. Rev. B* **53** 7504
[37] Zhong L, Wu R, Freeman A J and Olson G B 1997 *Phys. Rev. B* **55** 11133
[38] Kim M, Geller C B and Freeman A 2004 *J, Scr. Mater.* **50** 1341
[39] Fen Y Q and Wang C Y 2001 *Comput. Mater. Sci.* **20** 48
[40] Geng W T, Freeman A J, Wu R and Olson G B 2000 *Phys. Rev. B* **62** 6208
[41] Všianská M and Šob M 2011 *Prog. Mater. Sci.* **56** 817
[42] Janisch R and Elsässer 2003 *Phys. Rev. B* **67** 224101
[43] Zhang S, Kontsevoi O Y, Freeman A J and Olson G B 2011 *Phys. Rev. B* **84** 134104
[44] Wang Y B, Zhang G, Liu M J, Chen X L and Chen J 2009 *Chin. Phys. B* **18** 1181
[45] Zhang S J, Kontsevoi O Y, Freeman A J and Olson G B 2011 *Acta Mater.* **59** 6155
[46] Schmidt C, Ernst F, Finnis M W and Vitek V 1995 *Phys. Rev. Lett.* **75** 2160
[47] Grujicic M, Zhao H and Krasko G L 1997 *Int. J. Refract. Met. Hard Mater.* **15** 341
[48] Fuks D, Mundim K C, Liubich V and Dorfman S 1999 *Surf. Sci. Rev. Lett.* **6** 705
[49] Krasko G L 1993–1994 *Int. J. Refract. Met. Hard Mater.* **12** 251
[50] Dorfman S, Liubich V, Fuks D and Mundim K C 2001 *J. Phys.: Condens. Matter* **13** 6719
[51] Mikhailovskij I M, Sadanov E V, Mazilova T I, Dudka O V, Ksenofontov V A and Lugovska O I 2012 *Mater. Lett.* **70** 60
[52] Borovikov V, Tang X Z, Perez D, Bai X M, Uberuaga B P and Voter A F 2013 *Nucl. Fusion* **53** 063001
[53] Lee H and Tomar V 2013 *Comput. Mater. Sci.* **77** 131
[54] Zhou Y M, He Y G, Lu A X and Wan Q 2009 *Chin. Phys. B* **18** 3966
[55] Setyawan W and Kurtz R J 2012 *Scripta Mater.* **66** 558
[56] Zhang L, Fu C C and Lu G H 2013 *Phys. Rev. B* **87** 134107
[57] Zhou H B, Liu Y L, Jin S, Zhang Y, Luo G N and Lu G H 2010 *Nucl. Fusion* **50** 025016
[58] Kresse G, Hafner J 1993 *Phys. Rev. B* **47** 558
[59] Kresse G and Furthmüller J 1996 *Phys. Rev. B* **54** 11169
[60] Perdew J P, Burke K and Ernzerhof M 1996 *Phys. Rev. Lett.* **77** 3865
[61] Kong X S, You Y W, Song C, Fang Q F, Chen J L, Luo G N and Liu C S 2012 *J. Nucl. Mater.* **430** 270
[62] Rasch K D, Siegel R W and Schultz H 1980 *Philos. Mag. A* **41** 91
[63] McLean D 1957 *Grain Boundaries in Metals* (London: Oxford University Press)
[64] Bolt H, Barabash V, Krauss W, Linke J, Neu R, Suzuki S, Yoshida N and ASDEX Upgrade Team 2004 *J. Nucl. Mater.* **329–333** 66
[65] Fukuzumi S, Yoshiie T, Satoh Y, Xu Q, Mori H and Kawai M 2005 *J. Nucl. Mater.* **343** 308
[66] Rice J R and Wang J S 1989 *Mater. Sci. Eng.* **107** 23